RSC Advances

ROYAL SOCIETY OF CHEMISTRY

www.rsc.org/advances

Cite this: DOI: 10.1039/c0xx00000x

www.rsc.org/xxxxxx

ARTICLE TYPE

Covalent crosslinked polyelectrolyte complex membrane with high negative charges towards anti-natural organic matter fouling nanofiltration

Linglong Shan,[a] Hongxia Guo,*[,b] Zhenping Qin,[a] Naixin Wang,[a] Shulan Ji,[a] Guojun Zhang*[,a]

Received (in XXX, XXX) Xth XXXXXXXXX 20XX, Accepted Xth XXXXXXXXX 20XX
DOI: 10.1039/b000000x

Removal of natural organic matter (NOM) from drinking water by membrane technology is attracting increasing attention. However, the fouling of the membrane by NOM is one of the biggest obstacles restricting its widespread application. Therefore an anti-NOM fouling polyelectrolyte complex (PEC) membrane was obtained by creating a negatively charged multilayer on a polyacrylonitrile (PAN) supporting membrane using a layer-by-layer assembly method. To improve the stability of the PEC membrane, the electrostatically assembled (poly(ethyleneimine)/poly(sodium 4-styrenesulfonate))$_n$/PAN membranes were crosslinked by glutaraldehyde. It was found that the zeta potential of the membrane surface decreased after chemical crosslinking, which further improved the electrostatic repulsion to NOM and thus improved the anti-NOM fouling property. Results of a 30-day nanofiltration operation showed the crosslinked membrane had good stability and gave a higher rejection of NOM; the permeance of the crosslinked membrane was double that of the uncrosslinked membrane.

Introduction

Natural organic matter (NOM) in water, arising from the dissolution of dead and living organic matter in the hydrologic cycle, is an inevitable component in aquatic ecosystems. NOM is negatively charged and can be divided into three categories: humic acid (HA), fulvic acid (FA) and humin, with molecular weights ranging from <1 kDa to >500 kDa.[1-3] NOM can affect the odor, taste, and color of raw water. Moreover, in the process of water treatment, NOM can react with disinfectants to generate carcinogenic disinfection by-products (DBPs) such as trihalomethane and haloacetic acid.[4-8] Thus, the effective removal of NOM is crucial for domestic water use. Recently, membrane technologies, such as microfiltration (MF),[9, 10] ultrafiltration (UF)[11-16] and nanofiltration (NF)[14, 16-19] have been studied for removing NOM from raw water, because of the stringent regulations on drinking water quality.[13] In view of the small size of NOM, they can not be effectively removed by MF and UF technology.[14, 15] NF has been considered to be an effective way to remove NOM, due to its smaller pore size and the finely tuned charge on membrane surface.[16] However, the fouling of membrane caused by NOM can not be ignored. HA has been regarded as the most prominent NOM component. Fouling by HA adsorption on NF membrane surfaces often results in a low filtration flux. Therefore, decreasing the adsorption of HA on membrane surface has attracted much attention. Because NOM is negatively charged, the electrostatic repulsion negatively charged membranes have been considered as an effective way to reduce fouling. Song et al found that compared with the essentially neutral regenerated cellulose (RC) NF membrane, negatively charged RC NF membrane improved the rejection of HA and decreased the flux decline, due to the increase of electrostatic interaction between the charged HA and the charged membrane.[14] Lee et al. also found that negatively charged NF membranes provide better NOM removal and higher pure water permeability than uncharged membranes.[18] Zhao et al. prepared poly(N-isopropylacrylamide) brushes grafted with ZrO_2 composite NF membrane for HA removal. They found that high rejection and good anti-fouling performance were obtained when the electrostatic repulsion between HA and the membrane surface was strong.[20] So, fabricating a negatively charged membrane has proved an effective way to avoid membrane fouling of NOM and provide a high NOM removal rate.

Charged NF membranes have been fabricated by a few different methods, such as chemical crosslinking,[21] grafting,[22-24] phase inversion,[25] and layer-by-layer (LbL) assembling techniques.[26-31] Of these methods, the LbL technique is the simplest for the formation of ultrathin films of NF membranes with controlled thickness and interfacial properties.[26, 32-35] However, most studies have focused on the formation of charged multilayer films, considering aspects such as the composition of the polyelectrolyte solution, pH, and concentration.[36, 37] The long term performance of these polyelectrolyte membranes has often been neglected, which is critical for industrial application. It is well-known that real water treatment processes are usually relatively complicated. There is a possibility that the presence of salt, acid, alkali and oxidant in the feed solution would affect the stability of electrostatically assembled polyelectrolyte multilayer membranes.[38-40] Strengthening the binding force between the polyelectrolytes thus plays an important role in improving the stability of the polyelectrolyte membrane.

Therefore, a new strategy is proposed herein to prepare an anti-NOM fouling and highly stable nanofiltration membrane for water purification. As shown in Scheme 1, a negatively charged multilayer was assembled onto a polyacrylonitrile (PAN) ultrafiltration supporting membrane by alternate deposition of

poly(ethyleneimine) (PEI) and poly(sodium 4-styrenesulfonate) (PSS). To ensure the formation of the whole negatively charged multilayer, in addition to the deposition of the outermost layer with a negatively charged PSS, the concentration of the PEI solution was held much lower than that of the PSS solution during the LbL assembly. The whole as-prepared (PSS/PEI)n/PAN complex membrane was then crosslinked by glutaraldehyde (GA). The chemical compositions, charge properties and wettability of the multilayer membranes were intensively characterized using Fourier transform infrared (FTIR), X-ray diffraction (XRD), zeta potential, and contact angle analyzers. Micrographs of the complex membranes were recorded using scanning electron microscopy (SEM) and atomic force microscopy (AFM). The effects of the pH value of the PEI solution, the PSS concentration and assembly layer on nanofiltration performance were also investigated. Finally, the long-term NF performance and the anti-NOM fouling capacity of the membranes during the filtration of HA were investigated.

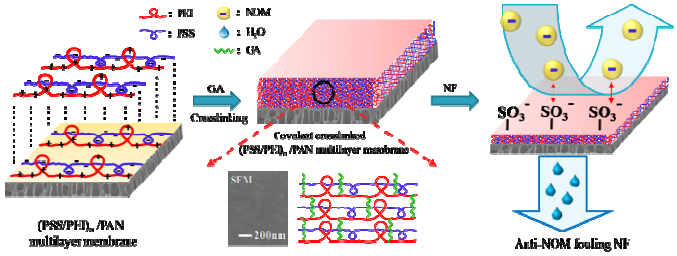

Scheme 1. Schematic illustration of the preparation of $(PSS/PEI)_{5.0}$/PAN multilayer membrane, covalent crosslinked $(PSS/PEI)_{5.0}$/PAN multilayer membrane and the NF operation.

Experimental

Chemicals and materials

A PAN UF membrane with molecular weight cutoffs of 100 kDa (PAN-50) was purchased from Sepro Membranes (Oceanside, CA, USA). Unless otherwise specified, all reagents and chemicals were analytical grade. HA, PEI (Mw=750,000) and PSS (Mw=1 000,000) were obtained from Aldrich (St. Louis, MO, USA). GA, hydrochloric acid (HCl), potassium chloride (KCl) and sodium hydroxide (NaOH) were provided by Beijing Chemical Factory (Beijing, China). All the chemicals were used as received without further purification. Deionized water was used for membrane rinsing and preparation of polyelectrolyte solutions.

Preparation of covalent crosslinked multilayer membrane

The $(PSS/PEI)_n$/PAN membrane and crosslinked $(PSS/PEI)_n$/PAN membrane were prepared as illustrated in Scheme 1. Firstly, in order to obtain a charged substrate, PAN was hydrolyzed with 2.0 mol/L NaOH and rinsed with deionized water. The negative charged PAN substrate was then immersed in 1.0 mg/mL of PEI polycation solution for 20 min, and rinsed with deionized water three times. The pH value of the PEI solution was adjusted by addition of HCl or NaOH within 1–11. Subsequently, to assemble PSS，the PEI/PAN membrane was immersed in 1.0–5.0 mg/mL of PSS polyanion solution for 20 min, and rinsed with deionized water again. This procedure was repeated until the required $(PSS/PEI)_n$/PAN polyelectrolyte multilayer obtained. The $(PSS/PEI)_n$/PAN membrane was then crosslinked by immersing it in 0.02 mg/mL GA aqueous solution at 30°C for 24 h. Lastly, the crosslinked membrane was rinsed with deionized water and dried in an oven at 30 °C, to produce the covalent crosslinked $(PSS/PEI)_n$/PAN membrane.

NF performance of the membranes

As per our previous study,[27] NF performance was studied with a home-made cross-flow NF system, which is shown in Scheme 2. The exposed active membrane area for filtration in the cell was 22.9 cm^2. HA aqueous solution (10 mg/L) was used as the typical model of natural water with NOM, pressurized with a diaphragm pump and maintained at 0.6 MPa. In the long-term NF operation tests, membranes were tested every few days, each time lasting about 2 hours, and then the membranes were dipped in 10 mg/L HA aqueous solution. HA concentration was measured using an ultraviolet-visible spectrophotometer (T6, Shanghai, China) at the maximal absorption wavelength of 254 nm. The rejection ratio, R, was calculated using Eq. (1), where C_f and C_p are concentrations of solutes in the feed and permeate, respectively. The permeability, J, was calculated by Eq. (2), where V is the volume of the permeate liquid, which was flowing across the membrane of area A (m^2) in the time period T (h) and operative pressure P (MPa).

$$R = (C_f - C_p)/C_f \times 100\% \quad (1)$$

$$J = V(L) \times A(m^2)^{-1} \times T(h)^{-1} \times P(MPa)^{-1} \quad (2)$$

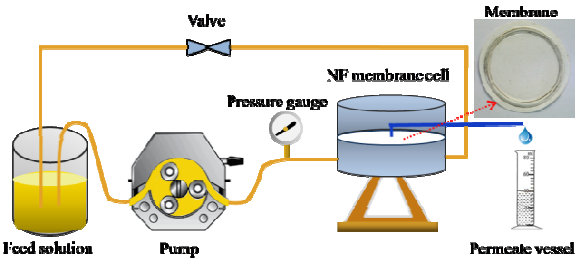

Scheme 2. Setup for nanofiltration experiments.

Characterization

Zeta potentials of the membranes were determined using a SurPASS electrokinetic analyzer (Anton Paar GmbH, Graz, Austria). During the process of measuring the zeta potential, the KCl solution concentration was maintained at 0.83 mmol/L, while the operation pressure was 0.03 MPa. The zeta potentials of HA solution and PEI solution were obtained by a laser scattering size analyzer (NICOMP ™ 380ZLS, USA). The pH values of the solutions were measured with a pH meter (Leici PHS-3C, Shanghai, China). Attenuated total reflectance FTIR spectra (TENSOR 27, Bruker, Germany) was used to characterize the chemical composition changes of the multilayer assembled on the PAN substrate. Wide-angle XRD experiments were conducted on a D8 ADVANCE X-ray diffractometer (Bruker/AXS, Germany). The membrane surface morphologies were observed via SEM (Hitachi SU-8020, Japan), with the microscope attached to an energy dispersive spectrometer (EDS). All membrane samples were dried under vacuum and fractured in liquid nitrogen. Surface topography was also observed by AFM in tapping mode

(Pico ScanTM 2500, USA). Water contact angle measurement was performed using a contact angle analyzer (DSA100, Germany).

Results and discussion

Charge property, chemical compositions and wettability of the multilayer membranes

Adjusting the surface charge is considered one of the main strategies for improving the anti-fouling properties of membranes. To monitor the electrical properties of the membranes, the surface zeta potentials were measured using an electrokinetic analyzer. Such measurements were also used to track the stepwise growth of sequential polyelectrolyte layers during the LbL assembly process.[42] The variations of the surface zeta potentials with different layers during the assembly process are shown in Fig. 1(a). It can be noted that the hydrolyzed PAN substrate had a negative charge of –61.0 mV. When deposited by the PEI solution, the zeta potential of the membrane surface increased to –19.0 mV, and then decreased to –64.0 mV due to the assembly of PSS; the zeta potentials of the membrane surface changed between –84.0 mV and –19.0 mV with further alternating assembly. Zeta potentials usually alternate between positive and negative after each polycation or polyanion adsorption, as has been demonstrated by many researchers.[27, 31, 38] However, in contrast to typical LbL assembly, the zeta potential in this study was always negative with the deposited multilayer. In a typical weak polyelectrolyte, the protonation degree of PEI varies with the pH value of the solution.[43] In this work, the PEI solution was

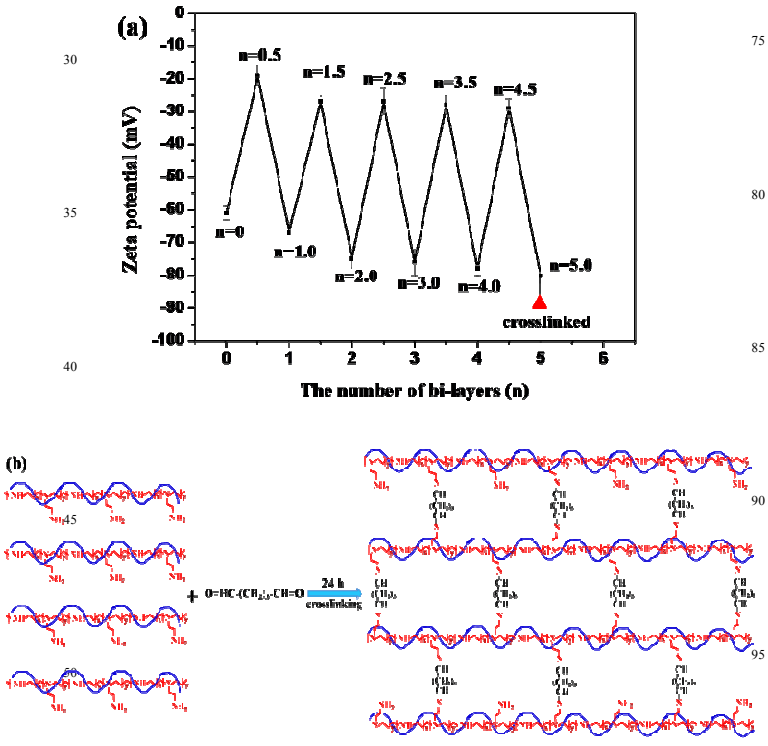

Fig. 1 (a) Zeta potentials of the membrane surfaces varied with a number of layers (Assembly conditions: PEI concentration 1.0 mg/mL, PSS concentration 2.0 mg/mL, PEI pH =1, PSS pH =7, required layers; crosslinking condition: 0.02 mg/mL of GA solution for 24 h.); (b) schematic crosslink reaction of polyelectrolytes with GA.

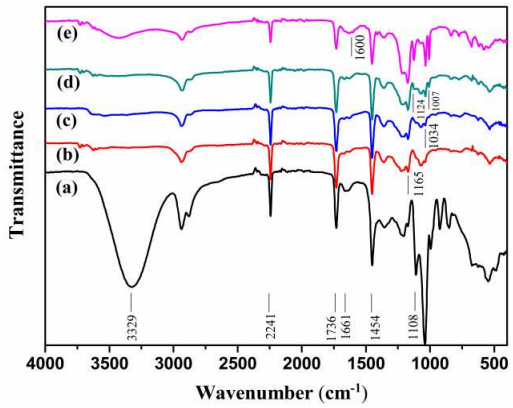

Fig. 2 ATR-FTIR spectra of (a) hydrolyzed PAN substrate, (b) $(PSS/PEI)_{0.5}$/PAN membrane, (c) $(PSS/PEI)_{1.0}$/PAN membrane, (d) $(PSS/PEI)_{5.0}$/PAN membrane, (e) crosslinked $(PSS/PEI)_{5.0}$/PAN membrane. (Assembly conditions: PEI concentration 1.0 mg/mL, PSS concentration 2.0 mg/mL, PEI pH =1, PSS pH =7, required layers; crosslinking condition: 0.02 mg/mL of GA solution for 24 h.)

adjustedto a low pH, while the PEI concentration was controlled as 1.0 mg/mL, which was much less than the PSS concentration (2.0 mg/mL). In this case, the polycation PEI mainly played a bridging agent role to ensure the successful assembly of the next PSS layer. Therefore, the deposition of PEI did not reverse the charge of the sub-layer, which ensured the whole multilayer was negatively charged during the LbL assembly. This strategy indicated the formation of a high negatively charged membrane can be tuned by the pH and concentration of polyelectrolytes. Furthermore, after being crosslinked by GA, the zeta potential of the membrane showed an apparent decrease from –80.0 mV to –88.4 mV in Fig. 1(a). The decreased zeta potential of the membrane was due to the reaction of $–NH_2$、–NH– with –CH=O. Fig. 1(b) shows the reaction of $–NH_2$ with GA.[21]

Attenuated total reflection-FTIR spectra were performed to verify the formation of the crosslinked PEC membrane. The FTIR spectra of the hydrolyzed PAN substrate, after assembly of $(PSS/PEI)_n$, as well as after crosslinking are shown in Fig. 2. The absorption at 3329 cm^{-1} was assigned to carboxyl –OH, which confirmed that some of the nitrile groups of PAN were hydrolyzed by NaOH solution (Fig. 2(a)).[44] After deposition of the polycationic PEI (Fig. 2(b)), the intensity of the absorption peak of C-N at 1165 cm^{-1} increased, which can be ascribed to the interaction between the amine of PEI and the carbonyl of hydrolyzed membrane. New signals, which appeared at 1124, 1034 and 1007 cm^{-1}, were due to sulfonate moieties in the deposited PSS polyanions (Fig. 2(c) and (d)).[30] Moreover, the new peak of C=N at 1600 $cm^{-1}$and the increased peak of C=O at 1661 cm^{-1} in Fig. 2(e) resulted from the crosslinking reaction of PEI with GA (Fig. 1(b)). It has been widely demonstrated previously that the structural organization of LbL-assembled multilayer such that they are interwoven.[26, 45-54] Therefore, the PEI migrated into the PSS layers. Obviously, the positively charged PEI and negatively charged PSS was electrostatically crosslinked. In this case, the nature of the crosslinking actually consists of both covalent and electrostatical crosslinking. Since the interwoven PEI/PSS multilayer may actually contain a continuous phase rather than discrete layers, the GA post-

treatment might lead to a very stable crosslinking structure. Wide-angle XRD was used to further examine the structural changes of the membranes before and after crosslinking (Fig. 3). Fig. 3(a) showed a wide and short peak of the crosslinked $(PSS/PEI)_{5.0}$/PAN membrane compared with that of the uncrosslinked one (Fig. 3(c)), indicating that the degree of crystallinity of the polyelectrolytes on membrane surface decreased after GA crosslinking. This might be attributed to the formation of more amorphous structure after crosslinking of polyelectrolytes. Then the formation of the interwoven structure restricted the activity of the polyelectrolyte chains. XRD of the crosslinked membrane and uncrosslinked membrane placed for 15 days in air was used to investigate the subsequent crystallinity variations (Fig. 3(b) and (d)). The crystallinity of the uncrosslinked membrane continuously increased while exposed to air. While the crystallinity of the crosslinked membrane remained unchanged.

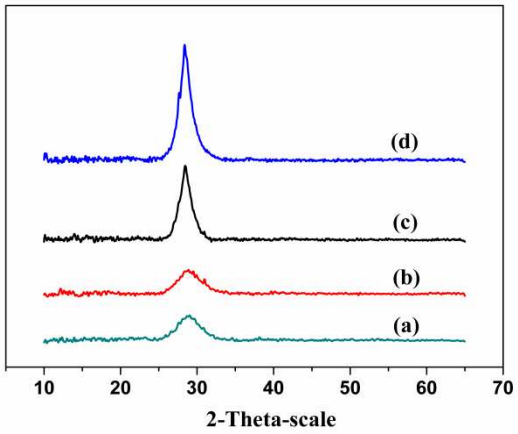

Fig. 3 XRD patterns of (a) crosslinked $(PSS/PEI)_{5.0}$/PAN membrane, (b) crosslinked $(PSS/PEI)_{5.0}$/PAN membrane after 15 days, (c) uncrosslinked $(PSS/PEI)_{5.0}$/PAN membrane, (d) uncrosslinked $(PSS/PEI)_{5.0}$/PAN membrane after 15 days. (Assembly conditions: PEI concentration 1.0 mg/mL, PSS concentration 2.0 mg/mL, PEI pH =1, PSS pH =7, five layers; crosslinking condition: 0.02 mg/mL of GA solution for 24 h.)

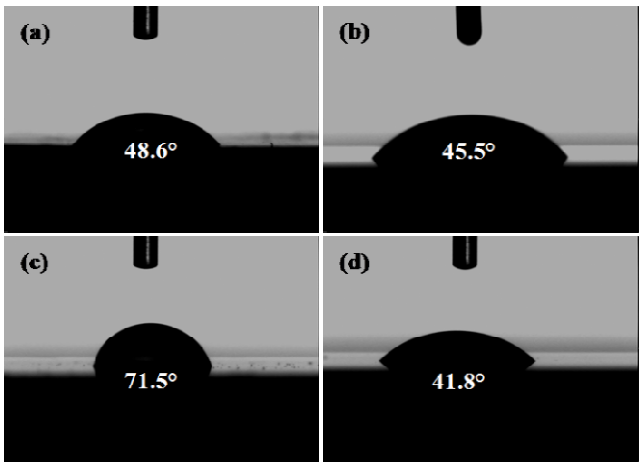

Fig. 4 Contact angles of (a) PAN substrate (48.6±0.08°), (b) $(PSS/PEI)_{3.0}$/PAN membrane (45.5±0.06°), (c) $(PSS/PEI)_{5.0}$/PAN membrane (71.5±0.12°), (d) crosslinked $(PSS/PEI)_{5.0}$/PAN membrane (41.8±0.22°) (Assembly conditions: PEI concentration 1.0 mg/mL, PSS concentration 2.0 mg/mL, PEI pH =1, PSS pH =7, required layers; crosslinking condition: 0.02 mg/mL of GA solution for 24 h.)

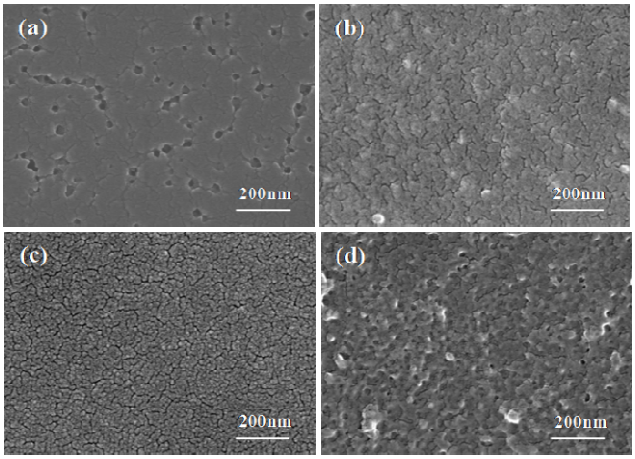

Fig. 5 SEM images of (a) PAN substrate, (b) $(PSS/PEI)_{3.0}$/PAN membrane, (c) $(PSS/PEI)_{5.0}$/PAN membrane, (d) crosslinked $(PSS/PEI)_{5.0}$/PAN membrane. (Assembly conditions: PEI concentration 1.0 mg/mL, PSS concentration 2.0 mg/mL, PEI pH =1, PSS pH =7, required layers; crosslinking condition: 0.02 mg/mL of GA solution for 24 h.)

Fig. 4 shows that the assembly of polyelectrolytes also changed the wettability of the membrane surface. The contact angle of PAN substrate was 48.6° (Fig. 4(a)), and it was almost unchanged after the deposition of 3.0 layers PSS/PEI (Fig. 4(b)). Then it showed an apparent increase to 71.5° when the number of assembly layers increased to 5.0 (Fig. 4(c)). Moreover, after being crosslinked, the contact angle decreased to 41.8° (Fig. 4(d)), due to the sharply decreased roughness (Fig. 6(d)), which might be preferred to prevent membrane fouling.[55-62]

Morphology and the thickness of the PEC membrane

The changes in the surface morphology revealed by SEM are shown in Fig. 5. From the high magnification images (100 k×), a large number of pores can be clearly observed on the PAN substrate (Fig. 5(a)). In contrast, after assembly with 3.0 layers PSS/PEI, most of the surface pores had been covered (Fig. 5(b)), and all the defects of PAN substrate had been covered when the layers of PSS/PEI increased to 5.0 (Fig. 5(c)). It was also clearly observed from Fig. 5(d) that the crosslinked polyelectrolytes endowed the membrane with remarkably high density and compactness.

AFM was also used to characterize the changes of the surface morphologies, as shown in Fig. 6. The square roughness (sqr) values were obtained based on a 100 μm×100 μm scan area. Significant changes were observed on the membrane surface. The surface of the PAN substrate showed a sqr value of 397.0 nm (Fig. 6(a)). After deposition of 3.0 layers PSS/PEI, the membrane surface was relatively flat with a sqr value of 26.5 nm (Fig. 6(b)). Then the surface turned much rougher with a sqr value of 876.0 nm after assembly with 5.0 layers PSS/PEI (Fig. 6(c)). However, the roughness decreased from 876.0 nm to 40.4 nm after crosslinking, as shown in Fig. 6(d). This might be attributed to the surface enrichment of crosslinked polyelectrolytes. Usually, lower roughness is better for the anti-NOM fouling properties of the membrane.[58, 61, 62]

In addition, the cross-section of the membrane was observed by SEM-EDS to analyze the thickness of the multilayer assembled.

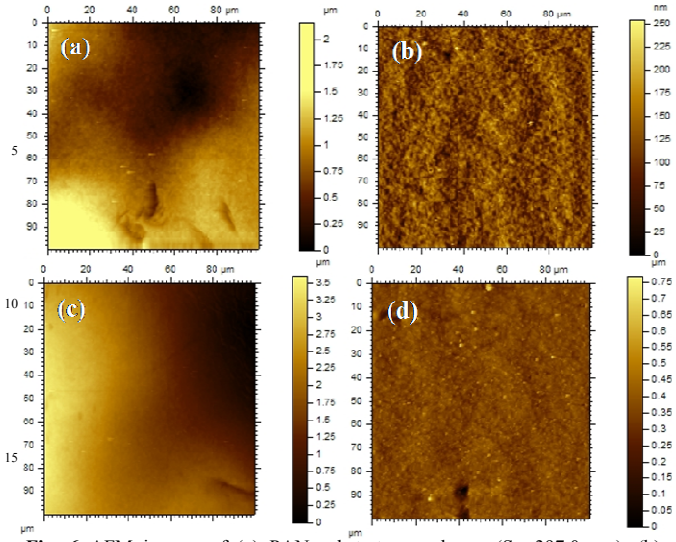

Fig. 6 AFM images of (a) PAN substrate membrane (Sq=397.0 nm), (b) $(PSS/PEI)_{3.0}$/PAN membrane (Sq=26.5 nm), (c) $(PSS/PEI)_{5.0}$/PAN membrane (Sq=876.0 nm), (d) crosslinked $(PSS/PEI)_{5.0}$/PAN membrane (Sq=40.4 nm). (Assembly conditions: PEI concentration 1.0 mg/mL, PSS concentration2.0 mg/mL, PEI pH =1, PSS pH =7, required layers; crosslinking condition: 0.02 mg/mL of GA solution for 24 h.)

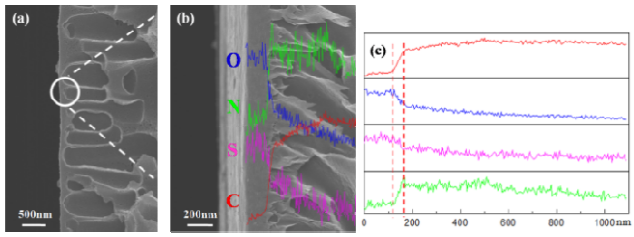

Fig. 7 SEM image and EDS analyses of the cross-section of $(PSS/PEI)_{5.0}$/PAN membrane. (Assembly conditions: PEI concentration 1.0 mg/mL, PSS concentration 2.0 mg/mL, PEI pH =1, PSS pH =7, five layers.)

From the cross-sectional SEM (Fig. 7(a)), it is difficult to obtain the exact thickness of the multilayer because there was no distinct boundary between the assembled multilayer and the substrate. Therefore, the changes of the elemental composition through the cross-section were further analyzed using EDS (Fig. 7(b) and (c)). Since the PAN substrate did not contain S while the PSS did, all S element must come from PSS. Therefore, variation of S element along the cross-section of the composite membrane could be used to determine the thickness of the separation layer. Before 120 nm (from the top layer) the concentrations of C, N, S, O elements were at almost constant values. From 120 nm to 170 nm (from the top layer), it was noted that the concentrations of S and O elements sharply decreased, while the concentrations of C and N elements increased after 120 nm. After 170 nm, nearly none of S element was found while the concentrations of C, N, O elements again almost stayed at constant values. From this analysis, the thickness of the $(PSS/PEI)_{5.0}$ layer was determined to be about 120 nm. Meanwhile, the depth of the polyelectrolytes intrusion into PAN substrate was about 50 nm.

Effects of pH value of PEI solution, PSS concentration and assembly layer

The effects of the pH value of PEI solution on NF performance of the membrane were studied, as shown in Fig. 8(a). Both the rejection and permeance decreased with increasing pH of PEI. The membrane prepared at low pH of PEI provided an effective separation for HA might due to the high protonation degree of amino group.[63] It was clear that the appropriate pH of PEI solution was 1.

The effects of the polyelectrolyte concentrations on NF performance of the membrane were investigated by keeping the PEI concentration at 1.0 mg/mL and pH of 1. As shown in Fig.

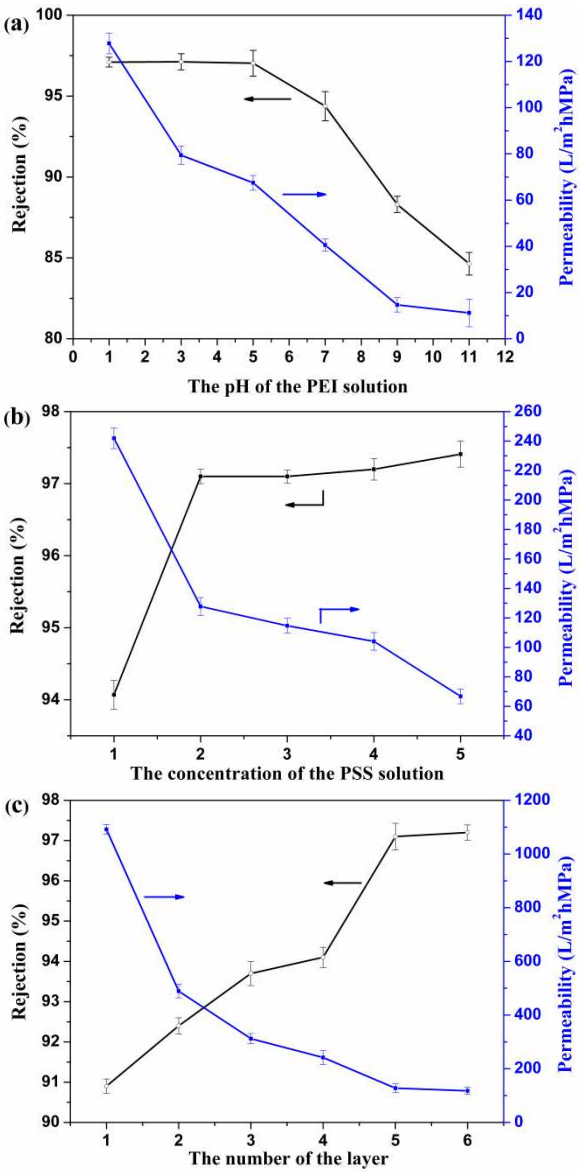

Fig. 8 (a) Effects of PEI pH on NF performance (Assembly conditions: PEI concentration 1.0 mg/mL, PSS concentration 2.0 mg/mL, PSS pH =7, five layers; operating conditions: 0.6 MPa, 10 mg/L HA solution.); (b) effects of PSS concentration on NF performance (Assembly conditions: PEI concentration 1.0 mg/mL, PEI pH =1, PSS pH =7, five layers; operating conditions: 0.6 MPa, 10 mg/L HA solution.); (c) effects of assembly layer on NF performance (Assembly conditions: PEI concentration 1.0 mg/mL, PSS concentration 2.0 mg/mL, PEI pH =1, PSS pH =7, required layers; operating conditions: 0.6 MPa, 10 mg/L HA solution.).

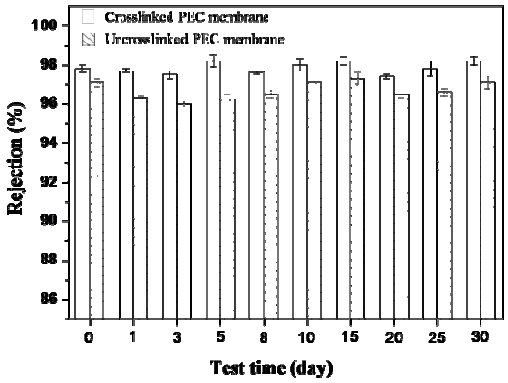

Fig. 9 Stability of uncrosslinked membrane and crosslinked membrane (Assembly conditions: PEI concentration 1.0 mg/mL, PSS concentration 2.0 mg/mL, PEI pH =1, PSS pH =7, five layers; crosslinking condition: 0.02 mg/mL of GA solution for 24 h; operating conditions: 0.6 MPa, 10 mg/L HA solution.).

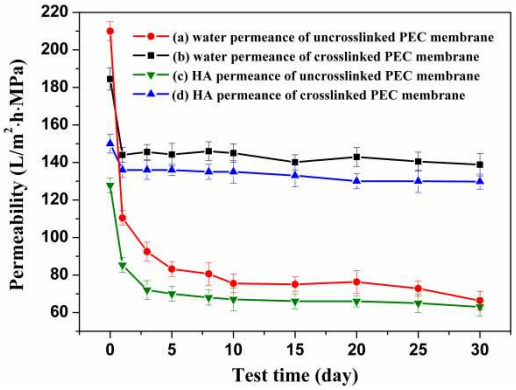

Fig. 10 Stability of uncrosslinked and crosslinked membrane. (a) water permeance of uncrosslinked $(PSS/PEI)_{5.0}$/PAN membrane. (b) water permeance of crosslinked $(PSS/PEI)_{5.0}$/PAN membrane. (c) HA permeance of uncrosslinked $(PSS/PEI)_{5.0}$/PAN membrane. (d) HA permeance of crosslinked $(PSS/PEI)_{5.0}$/PAN membrane. (Assembly conditions: PEI concentration 1.0 mg/mL, PSS concentration 2.0 mg/mL, PEI pH =1, PSS pH =7, five layers; crosslinking condition: 0.02 mg/mL of GA solution for 24 h; operating conditions: 0.6 MPa, 10 mg/L HA solution.).

8(b), the rejection increased and HA permeance decreased with the increase of PSS concentration. The rejection increased from 94.1% to 97.4% and HA permeance decreased from 241.9 L/(m^2·h·MPa) to 66.8 L/(m^2·h·MPa) when the PSS concentrations varied from 1.0 mg/mL to 5.0 mg/mL. A high concentration of PSS could decrease the zeta potential of membrane surface and promote the formation of a more compact separation layer. This could increase the electrostatic repulsion with HA to produce a better rejection and make the permeance decline. Considering both rejection and permeance, in subsequent experiments, 1.0 mg/mL and 2.0 mg/mL were selected as the appropriate PEI and PSS concentrations for the assembly process, respectively.

The NF performance of the membranes with different assembly layers was investigated in Fig. 8(c). With assembly layers increased from 1.0 to 6.0, the rejection of the membranes increased from 90.9% to 97.2%. Meanwhile, the HA permeance decreased from 1091.7 L/(m^2·h·MPa) to 118.0 L/(m^2·h·MPa).

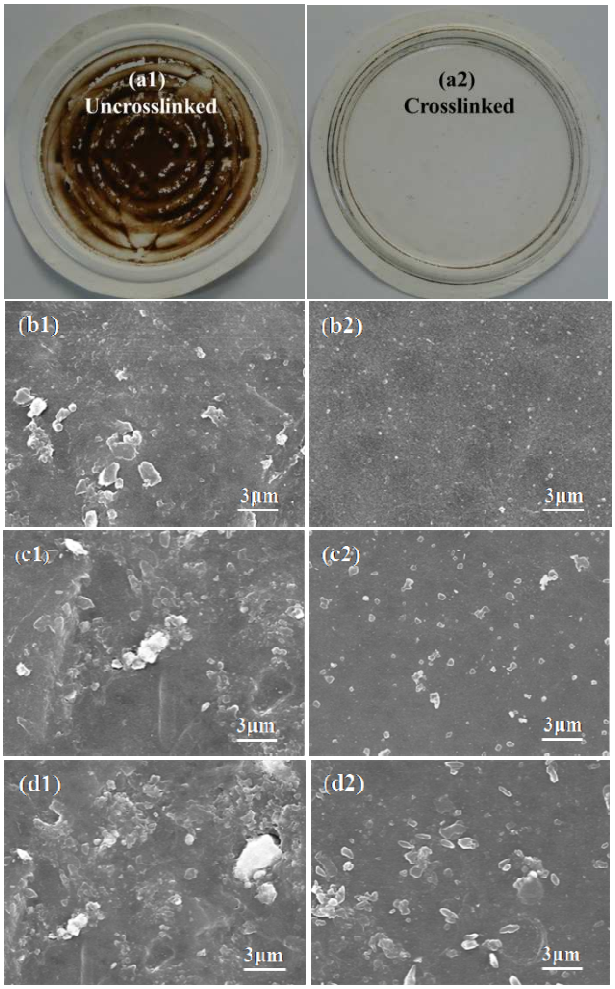

Fig. 11 Photographs of (a1) uncrosslinked $(PSS/PEI)_{5.0}$/PAN membrane and (a2) crosslinked $(PSS/PEI)_{5.0}$/PAN membrane, tested for 30 days. SEM images of (b1) uncrosslinked $(PSS/PEI)_{5.0}$/PAN membrane and (b2) crosslinked $(PSS/PEI)_{5.0}$/PAN membrane, tested for 1 day; (c1) uncrosslinked $(PSS/PEI)_{5.0}$/PAN membrane and (c2) crosslinked $(PSS/PEI)_{5.0}$/PAN membrane, tested for 10 days; (d1) uncrosslinked $(PSS/PEI)_{5.0}$/PAN membrane and (d2) crosslinked $(PSS/PEI)_{5.0}$/PAN membrane, tested for 30 days. (Assembly conditions: PEI concentration 1.0 mg/mL, PSS concentration 2.0 mg/mL, PEI pH =1, PSS pH =7, five layers; crosslinking condition: 0.02 mg/mL of GA solution for 24 h; operating conditions: 0.6 MPa, 10 mg/L HA solution.).

This is due to a more compact separation layer being formed along with the increase of assembled layers. Considering the compromise of the rejection and permeance, the appropriate assembly layer was selected as 5.0.

Long-term stability and anti-NOM fouling capacity

Our subsequent experiments were intended to examine the stability and anti-NOM capacity of the assembled membranes. The NF performances of the uncrosslinked and the crosslinked $(PSS/PEI)_{5.0}$/PAN membranes for separation of HA were analyzed for 30 days. As shown in Figs. 9 and 10, the rejection of the crosslinked membrane remained at 98.0±0.3% (Fig. 9(a)), which was higher than the uncrosslinked membrane (96.5±0.4%) (Fig. 9(b)). The initial water permeance of the uncrosslinked

membrane was 210.0 L/(m^2·h·MPa) (Fig. 10(a)), and the new crosslinked membrane decreased to 184.5 L/(m^2·h·MPa) (Fig. 10(b)) because of the formation of a denser separation layer. We can see that the water permeance of the uncrosslinked membrane decreased sharply to 110.4 L/(m^2·h·MPa), an approximately 50% decrease, after just dipping in the HA solution for one day, whereas the water permeance of the crosslinked membrane decreased to 144.0 L/(m^2·h·MPa). After 30 days use, the water permeance of the crosslinked membrane was 138.8 L/(m^2·h·MPa), double that of the uncrosslinked membrane (66.3 L/(m^2·h·MPa)). This indicated that the crosslinked membrane was more stable than the uncrosslinked one. The same phenomenon occurred for the HA permeance of uncrosslinked and crosslinked membranes (Fig. 10(c) and (d)). The permeance decline of the uncrosslinked membrane might be attributed to the continuous increase of the polyelectrolytes crystallinity (Fig. 3(c) and (d)) and the presence of more foulants on the membrane surface (Fig.11 (a1)). Although crosslinking post-treatment led to some permeance loss of the membrane at first, it also endowed the membrane with less permeance decline and higher rejection. These results proved that crosslinking post-treatment could give the polyelectrolyte membranes higher rejection and good stability performance. Meanwhile, as shown in Figs. 11(a1) and (a2), for uncrosslinked membrane, the color of membrane surface changed from white to brown black due to the heavy NOM fouling. As a comparison, the crosslinked membrane exhibited better anti-NOM fouling properties than the uncross-linked membrane at the macro level. Observations of the membrane top surface by SEM after NF operation for 1 day, 10 days and 30 days were conducted to further inspect fouling on the membrane surfaces. As shown in Fig. 11(b1), (c1) and (d1), the foulants on the surface of the uncrosslinked membrane became more and more obvious as the operation time progressed. Meanwhile, less pollutant was found on the crosslinked membrane surface at the same operation times (Fig. 11(b2), (c2), and (d2)). This might be ascribed to the presence of more negative charges on the surface of the crosslinked membrane (Fig.1a), and the stronger electrostatic repulsion of the membrane with HA leading to less deposition on the membrane surface.[60, 62] Also a low roughness and more hydrophilic surface of crosslinked membrane plays an important role. Thus the crosslinked membrane showed better anti-NOM fouling property than the uncrosslinked one.

Conclusions

In this study, a negatively charged, anti-NOM fouling and high stable membrane was developed by combining LbL-assembly and crosslink post-treatment. FTIR and XRD pattern confirmed the successful deposition of polyelectrolytes and an interwoven crosslinking structure. Zeta potential and contactangle analyses demonstrated that a much more negatively charged and hydrophilic surface was formed after chemical crosslinking. SEM and EDS analyses confirmed that the polyelectrolytes entered into the substrate pores and that the multilayer thickness is about 120 nm. NF experimental results demonstrated that the performance of membrane was strongly dependent on the polyelectrolytes pH, concentration and assembly layer. A set of appropriate conditions was selected as follows: PEI concentration 1.0 mg/mL, PSS concentration 2.0 mg/mL, PEI pH =1, PSS pH =7, five layers. With this set of given conditions, the $(PSS/PEI)_{5.0}$/PAN membrane obtained had a rejection of 97.1% and a water permeance of 210.0 L/(m^2·h·MPa) for the NF operation of 10 mg/L HA solution. The long-term experiments conducted over 30 days suggested that the crosslinked membrane showed an excellent stability and anti-NOM fouling capacity. The HA rejection could remain at 98.0±0.3% and the water permeance was maintained at 138.8 L/(m^2·h·MPa) after 30 days of NF operation, which were much higher than the 96.5±0.4% and 66.3 L/(m^2·h·MPa) values of the uncrosslinked membrane. In view of the versatile species of the charged polymer and customizable chemical functionalities, it is believed that this technology may contribute to the design and assembly of various charged membranes aimed at different foulants and thus extend the use of these membranes to different water and wastewater purifications.

Acknowledgments

This work was supported by the Natural Science Foundation of Beijing, China (8122010), the National Natural Science Foundation of China (21176005), and the Specialized Research Fund for the Doctoral Program of Higher Education (No. 20121103110010).

Notes and references

[a]*Center for Membrane Technology, College of Environmental and Energy Engineering, Beijing University of Technology, Beijing 100124, P. R. China. Fax:+86-10-67392393; Tel: +86 67392393;E-mail:zhanggj@bjut.edu.cn(G. Zhang).*

[b]*College of Material Science and Engineering, Beijing University of Technology, Beijing 100124, P. R. China. Fax:+86-10-67396110; Tel: +86 67396110;E-mail:hxguo@bjut.edu.cn(H. Guo).*

1 M. Jaouadi, N. Amdouni, and L. Duclaux, Desalination, 2012, 305, 64-71.
2 M. Ng, S. Liu, C.W.K. Chow, M. Drikas, R. Amal, and M. Lim, J. Hazard. Mater., 2013, 263, 718-725.
3 N.H. Lee, G. Amy, J.-P. Croué, and H. Buisson, Water Res., 2004, 38, 4511-4523.
4 S.W. Krasner, H.S. Weinberg, S.D. Richardson, S.J. Pastor, R. Chinn, M.J. Sclinenti, G.D. Onstad, and A.D. Thruston, Environ. Sci. Technol., 2006, 40, 7175-7185.
5 A.W. Zularisam, A.F. Ismail, and R. Salim, Desalination, 2006, 194, 211-231.
6 J. Wenk, M. Aeschbacher, E. Salhi, S. Canonica, U.V. Gunten, and M. Sanders, Environ. Sci. Technol., 2013, 47, 11147-11156.
7 M. Clever, F. Jordt, R. Knauf, N. Rabiger, R. Rudebusch, and H. Scheibel, Desalination, 2000, 131, 325-336.
8 J. C. Rojas, J. Pérez, G. Garralón, F. Plaza, B. Moreno, and M.A. Gómez, Desalination, 2011, 266, 128-133.
9 W. Yuan, and A.L. Zydney, J. Membr. Sci., 1999, 157, 1-12.
10 N. Ma, Y. Zhang, X. Quan, X. Fan, and H. Zhao, Water Res., 2010, 44, 6104-6114.
11 J. Lowe, and M.M. Hossain, Desalination, 2008, 218, 343-354.
12 P.D. Peeva, A.E. Palupi, and M. Ulbricht, Sep. Purif. Technol., 2011, 81, 124-133.
13 J. Shao, J. Hou, and H. Song, Water Res., 2011, 45, 473-482.
14 H. Song, J. Shao, Y. He, J. Hou, and W. Chao, J. Membr. Sci., 2011, 376, 179-187.
15 A. Mehrpavar, A. Rahimpour, and M. Jahanshahi, J. Taiwan InstChem E., 2014, 45, 275-282.
16 J. Cho, G. Amy, and J. Pellegrino, Water Res., 1999, 33, 2517-2526.
17 A.S. Al-Amoudi, Desalination, 2010, 259, 1-10.

18 S. Lee, J. Moon, S.-K. Yim, S.-H. Moon, and J. Cho, Desalination, 2002, 147, 237-241.
19 L.D. Nghiem, D. Vogel, and S. Khan, Water Res., 2008, 42, 4049-4058.
20 Y. Zhao, S. Zhou, M. Li, A. Xue, Y. Zhang, J. Wang, and W. Xing, Water Res., 2013, 47, 2375-2386.
21 D.A. Musale, andA. Kumar, Sep. Purif. Technol., 2000, 21, 27-37.
22 P.S. Zhong, N. Widjojo, T-S. Chung, M. Weber, and C. Maletzko, J. Membr. Sci., 2012, 417-418, 52-60.
23 X. Wang, J. Wei, Z. Dai, K. Zhao, and H. Zhang, Desalination, 2012, 286, 138-144.
24 A. Akbari, S. Desclaux, J.C. Remigy, and P. Aptel, Desalination, 2002, 149, 101-107.
25 I.-C. Kim, H.-G. Yoon, and K.-H. Lee, J. Appl. Polym. Sci., 2002, 84, 1300-1307.
26 G. Decher, Science, 1997, 277, 1232-1237.
27 Z. Qin, C. Geng, H. Guo, Z. Du, G. Zhang, and S. Ji, J. Mater. Res., 2013, 28 1449-1457.
28 B.W. Stanton, J.J. Harris, M.D. Miller, and M.L. Bruening, Langmuir, 2003, 19 7038-7042.
29 S.U. Hong, and M.L. Bruening, J. Membr. Sci., 2006, 280, 1-5.
30 X. Li, S.D. Feyter, D. Chen, S. Aldea, P. Vandezande, F.D. Prez, and I.F.J. Vankelecom, Chem. Mater., 2008, 20, 3876-3883.
31 N. Wang, S. Ji, G. Zhang, J. Li, and L. Wang, Chem. Eng. J., 2012, 213, 318-329.
32 M. Elzbieciak, S. Zapotoczny, P. Nowak, R. Krastev, M. Nowakowska, and P. Warszyński, Langmuir, 2009, 25, 3255-3259.
33 R. H. Lajimi, E. Ferjani, M.S. Roudesli, and A. Deratani, Desalination, 2011, 266, 78-86.
34 G. Zhang, H. Yan, S. Ji, and Z. Liu, J. Membr. Sci., 2007, 292, 1-8.
35 G. Zhang, W. Gu, S. Ji, Z. Liu, Y. Peng, and Z. Wang, J. Membr. Sci., 2006, 280, 727-733.
36 S. Abdu, M.-C. Martí-Calatayud, J. E. Wong, M. García-Gabaldón, and M. Wessling, Appl. Mater. Interfaces., 2014, 6, 1843–1854.
37 G. Liu, D. M. Dotzauer and M. L. Bruening, J. Membr. Sci., 2010, 354, 198–205.
38 N. Wang, G. Zhang, S. Ji, Z. Qin, and Z. Liu, J. Membr. Sci., 2010, 354, 14-22.
39 A. Escoda, P. Fievet, S. Lakard, A. Szymczyk, and S. Déon, J. Membr. Sci., 2010, 347, 174-182.
40 Y. Ji, Q. An, Q. Zhao, H. Chen, J. Qian, and C. Gao, J. Membr. Sci., 2010, 357 80-89.
41 H.W. Jomaa, and J.B. Schlenoff, Macromolecules, 2005, 38, 8473-8480.
42 F. Caruso, and H. Mohwald, J. Am. Chem. Soc., 1999, 121, 6039-6046.
43 Z. Adamczyk, A. Bratek, B. Jachimska, T. Jasimski, and P. Warszyń ski, J. Phys. Chem., 2006, 110, 22426-22435.
44 R. Malaisamy, A. Talla-Nwafo, and K.L. Jones, Sep. Purif. Technol., 2011, 77, 367-374.
45 G. Decher, and J. Schmitt,Prog. Colloid Polym. Sci., 1992, 89, 160-164.
46 G. Decher, Y. Lvov, and J.Schmitt,Thin Solid Films, 1994, 244, 772-777.
47 J. Schmitt, T. Gruenewald, G. Decher, P.S. Pershan, K. Kjaer, and M. Loesche, Macromolecules, 1993, 26, 7058-7063.
48 D. Korneev, Y. Lvov, G. Decher, J. Schmitt, and S.Yaradaikin, Physica B, 1995, 213-214, 954-956.
49 X. Zhang, Y.P. Sun, M.L. Gao, X.X. Kong, and J.C.Shen, Macromol. Chem. Phys., 1996, 197, 509-515.
50 P. Fischer, M. Koetse, A. Laschewsky, E. Wischerhoff, L. Jullien, A. Persoons, and T. Verbiest, Macromolecules, 2000, 33, 9471-9473.
51 E.R. Kleinfeld, and G.S. Ferguson, Science, 1994, 265, 370-373.
52 J. Dai, D.M. Sullivan, and M.L. Bruening, Ultrathin, layered polyamide and polyimide coatings on aluminum, Ind. Eng. Chem. Res., 2000, 39, 3528-3535.
53 J.H. Choi, Y.W. Park, T.H. Park, E.H. Song, H.J. Lee, H. Kim, S.J. Shin, V.L.C. Fai, and B.-K. Ju, Langmuir, 2012, 28, 6826-6831.
54 H. Ajiro, K. Beckerle, J. Okuda, and M. Akashi, Langmuir, 2012, 28, 5372-5378.
55 A. Nabe, E. Staude, and G. Belfort, J. Membr. Sci., 1997, 133, 57-72.
56 Y. Chen, Q. Deng, J. Xiao, H. Nie, L. Wu, W. Zhou, and B. Huang, Polymer, 2007, 48, 7604-7613.
57 Z.-W. Dai, L.-S. Wan, and Z.-K. Xu, J. Membr. Sci., 2008, 325, 479-485.
58 J.-H. Li, Y.-Y. Xu, L.-P. Zhu, J.-H. Wang, and C.-H. Du, J. Membr. Sci., 2009, 326, 659-666.
59 H. Susanto, and M. Ulbricht, Langmuir, 2007, 23, 7818-7830.
60 C.X. Liu, D.R. Zhang, Y. He, X.S. Zhao, and R. Bai, J. Membr. Sci., 2010, 346, 121-130.
61 A. Tiraferri, Y. Kang, E.P. Giannelis, and M. Elimelech, Environ. Sci. Technol., 2012, 46, 11135-11144.
62 Y. Chang, Y.-J. Shih, R.-C. Ruaan, A. Higuchi, W.-Y. Chen, and J.-Y. Lai, J. Membr. Sci., 2008, 309, 165-174.
63 J. Suh, H.-J. Paik, and B. Hwang, Bioorg. chem., 1994, 22, 318-327.